









Single-Phase Grid and Solar PV Integration with 15-Level Asymmetrical Multilevel Inverter

Asapu Siva¹ , Y. T. R. Palleswari¹ , Kalyan Sagar Kadali¹ ,
Ramu Bhukya¹ , Mamatha Deenakonda² , and V. V. Vijetha Inti² 

¹ Department of Electrical and Electronics Engineering,
Shri Vishnu Engineering College for Women (Autonomous), Bhimavaram, Andhra Pradesh,
India

asivae@svcew.edu.in

² Department of Electrical and Electronics Engineering, Vishnu Institute of Technology,
Bhimavaram, Andhra Pradesh, India

Abstract. In the modern era of renewable energy generation and distribution, injecting solar power into the utility grid has gained universal recognition, also solar energy plays a crucial role for smart cities development. Grid-connected asymmetrical multilevel inverters have undergone significant development for integrating solar into the utility grid. This article aims to implement a 15-level asymmetrical inverter in a single-phase grid-integrated PV system and analyses the proposed system working with a 15-level inverter. This inverter topology has fewer switching devices, design with three DC sources and can generate fifteen output voltage levels; in this proposed system, these three DC sources are designed by three PV modules and three conventional boost converters. P&O (Perturb and Observe) Algorithm was implemented on each boost converter to extract the maximum power from three PV modules. The proposed system is simulated in MATLAB 2023a with toolboxes. The simulation results show whether the inverter can export the power to the grid under various solar irradiance conditions. The solar-based proposed system is well suited for groups of houses in smart cities.

Keywords: Photovoltaic (PV) · Multilevel inverter (MI) · MPPT · Smart cities

1 Introduction

Day by day, smart cities grow, and their power demand also increases day by day. As cities try to become “smart,” clean energy sources like solar and wind can be a big part of helping them reach their goals and demand [1]. Solar photovoltaic (PV) systems are growing in popularity as distributed generators around the world due to their low environmental impact. PV panels have become much more affordable, but the DC power they typically produce is unstable. Therefore, DC-DC or DC-AC conversions are necessary before the PV power can be fed to the output load or connected to the grid power [2, 3].

Solar energy can be integrated with the load or grid in one of two ways: a single-stage [4] or two-stage process [5, 6]. In [7], a two-stage, single-phase PV system is presented that can function independently of batteries. In order to regulate a two-stage power system, a proportional-integral (PI) design was presented in the article [8]. Inverters play a crucial role in transforming the DC output of solar panels into the AC current used by the grid [9]. In-depth research has been done on the asymmetrical inverters for PV systems in the literature [10, 11].

This article aims to implement a 15-level asymmetrical inverter in a single-phase grid-integrated PV system and observe the performance of the proposed system when 15-level inverters are used in the single-phase grid-integrated PV system. This 15-level inverter was proposed [12] by Marif Daula Siddique. A grid-connected PV system (GCPVS) with a two-power stage, single phase, and no transformer is depicted in circuit diagram form in Fig. 1.

The proposed system, including the boost converter design and PV system design, is presented in Sect. 2. Section 3 of the paper explains a maximum power point tracking (MPPT) and inverter control. Simulation results for the proposed multilevel inverter are presented in Sect. 4. Section 5 provides a conclusion.

2 Proposed System

2.1 Main Circuit

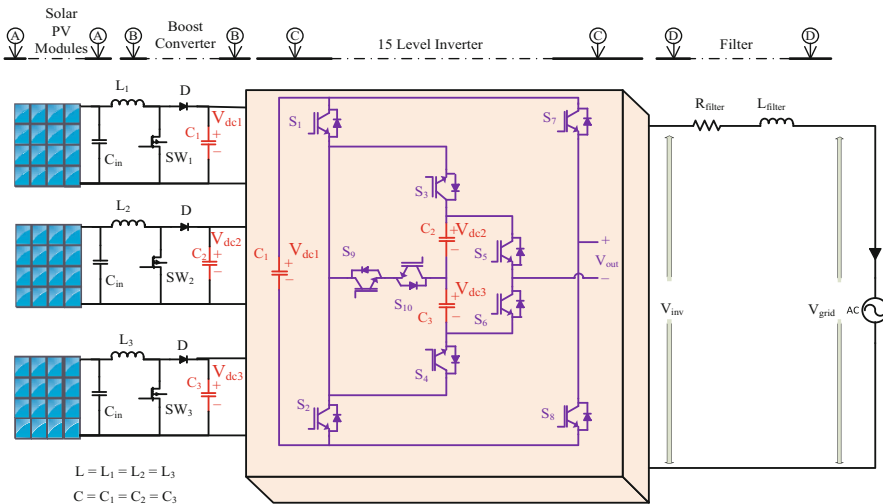


Fig. 1. Proposed System

Figure 1 depicts a schematic diagram of a two-stage conversion system. The circuit mainly consists of three DC-DC converters, 15 level inverter and a solar PV system. They are made to last long and withstand the harshest environmental conditions. In this system, three PV modules are connected to 15 level inverter as DC voltage sources via three boost converters and an inverter connected to the grid through filters.

2.2 15-level Inverter

The 15-level inverter switching states are shown in Table 1 (Table 2).

Table 1. Switches ON states

S.NO	ON state Switches				Vout
1	S ₂	S ₃	S ₇	S ₆	350V
2	S ₁	S ₃	S ₆	S ₇	300V
3	S ₁	S ₃	S ₆	S ₈	250V
4	S ₂	S ₆	S ₇	S ₉	200V
5	S ₁	S ₆	S ₇	S ₉	150V
6	S ₁	S ₆	S ₈	S ₉	100V
7	S ₂	S ₄	S ₆	S ₇	50V
8	S ₁	S ₃	S ₅	S ₇	0V
9	S ₁	S ₃	S ₅	S ₈	-50V
10	S ₂	S ₅	S ₇	S ₉	-100V
11	S ₂	S ₅	S ₈	S ₉	-150V
12	S ₁	S ₅	S ₈	S ₉	-200V
13	S ₂	S ₄	S ₅	S ₇	-250V
14	S ₂	S ₄	S ₅	S ₈	-300V
15	S ₁	S ₄	S ₅	S ₈	-350V

Table 2. PV Module parameters.

S.NO	PV Module's parameters	Values
1	current (short-circuit)	7.84A
2	voltage (open-circuit)	41 V
3	PV Current (at maximum point)	7.35 A
4	PV Voltage (at maximum point)	33 V
5	Power (at maximum point)	242.5 W
6	current (short-circuit)	7.84 A

2.3 The PV Array

The inverter in this system needs three DC power sources, and they all have different voltage ratings. Three Solar PV modules and three DC-DC boost converters were used to make these three DC power sources. As a DC source, each DC-DC boost converter is linked to a single 250 W PV module. Solar PV module design is carried out by simulating the environment’s natural conditions, which are then processed to produce the voltage vs current at different irradiance and voltage vs power at different irradiance graphs. Table 1 shows the parameters of the solar module. Figure 2 shows the curves of the solar module panel.

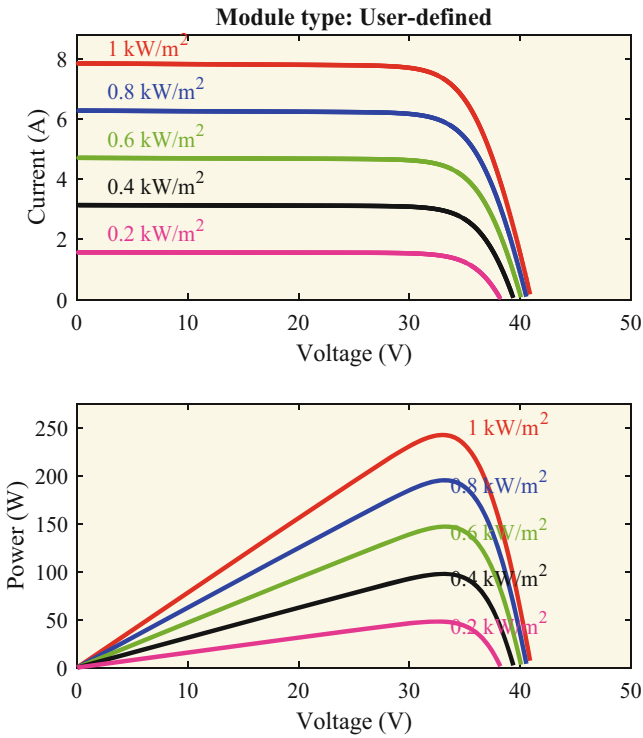


Fig. 2. Characteristics Curve of a PV module

2.4 Design of the DC-DC Converter

In the proposed system, three boost converters are used, and each boost converter’s input voltage ranges from 25 V to 35 V. However, each boost converter’s output voltage depends on its duty ratios and inverter input voltages ($V_{dc1} = 50$ V, $V_{dc2} = 150$ V, and $V_{dc3} = 150$ V). Consider the boost converter’s switching frequency, current ripple, voltage ripple and load capacity to be 50 kHz, 5%, 5% and 250 W, respectively. The

inductance and capacitance are calculated as:

$$L = \frac{V_{in}(V_{out} - V_{in})}{f_{sw} \times \Delta I \times V_{out}} = 10.2 \text{ mH}$$

$$C = \frac{I_{out}(V_{out} - V_{in})}{f_{sw} \times \Delta V \times V_{out}} = 520 \text{ } \mu\text{H}$$

3 The Control System

The proposed system contains control strategies. One control strategy is for controlling boost converter output voltages, and the second is for controlling the inverter to export the power to the grid. The inverter control strategy should, however, include the following: 1) grid synchronization and 2) active power transfer by managing grid-injected current.

3.1 MPPT Algorithm

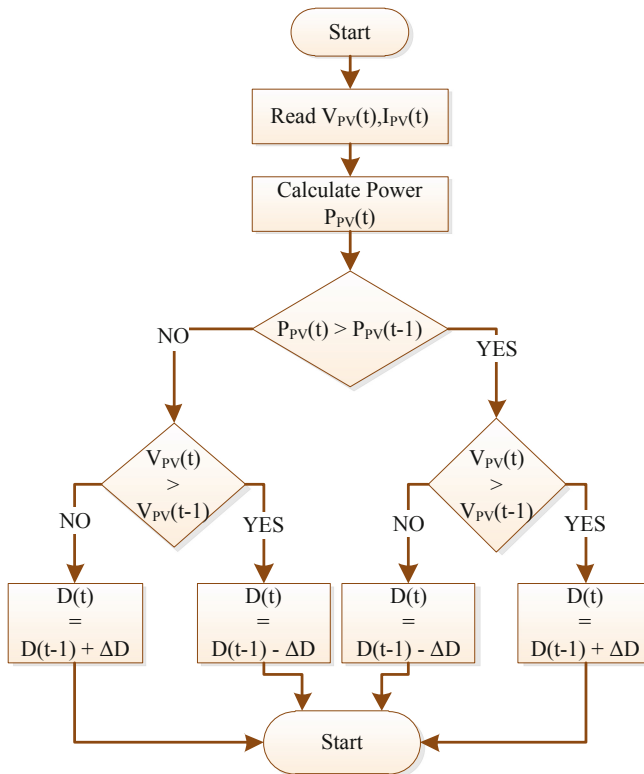


Fig. 3. MPPT controller

To track the maximum power from each solar module, the perturb and observe (P&O) algorithm is used for each module. Figure 3 is a flowchart illustrating the MPPT algorithm used to track the PV modules’ maximum power point. It compares the sampled value of the voltage to the previous value in the same way and sets the maximum point’s power duty according to the matching power’s result (Fig. 4).

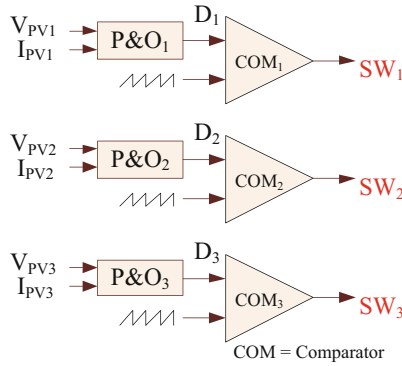


Fig. 4. Duty cycle control algorithm.

3.2 Control Technique for Inverter

A method known as Proportional Resonance Current (PRC) regulation is used to regulate the current flowing through the grid. The output of the PLL is multiplied to generate the reference current (i_{grid}^*), which is then compared to the measured Grid current (i_{grid}). In order to produce an appropriate reference signal under varying grid voltage, the PRC controller’s output maximises the current. The required gating signals for 10 switches are obtained by comparing measured grid voltage (V_{grid}) and reference voltage (V_L^*) (Fig. 5).

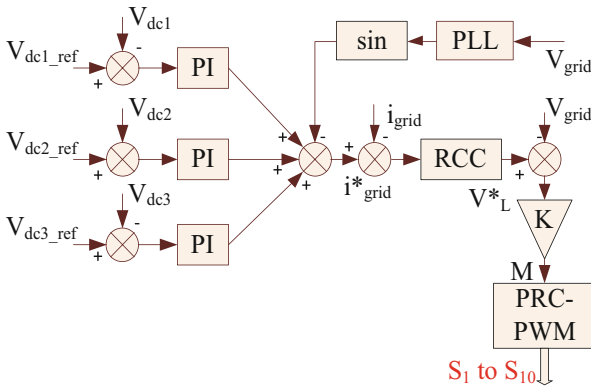


Fig. 5. Control technique for inverter

4 The Result Analysis

The process model and technique shown in Fig. 1 were verified through simulation studies. To examine the performance of the proposed system, two scenarios were simulated based on the model shown in Figs. 6, 7, 8 and 9

4.1 Proposed System Performance when Solar Irradiance Increases from 200 W/m² to 600 W/m²

At $t = 2$ s, The solar power generation increased from 140 w to 290 w as the solar irradiance increased from 200 w/m² to 400 w/m². The asymmetrical inverter can export 140 w power at 200 w/m² irradiance and 290 w power at 400 w/m² to the grid shown in Fig. 6(d). The boost converters maintain the output voltages as input to the inverter for successful operation. At $t = 3$ s, with an increase in solar irradiance from 400 W/m² to 600 W/m², solar power generation increased from 290 w to 440 w and the same amount of power was exported to the grid by the inverter. It has been observed that as the solar irradiance increases, the inverter can export power to the utility grid.

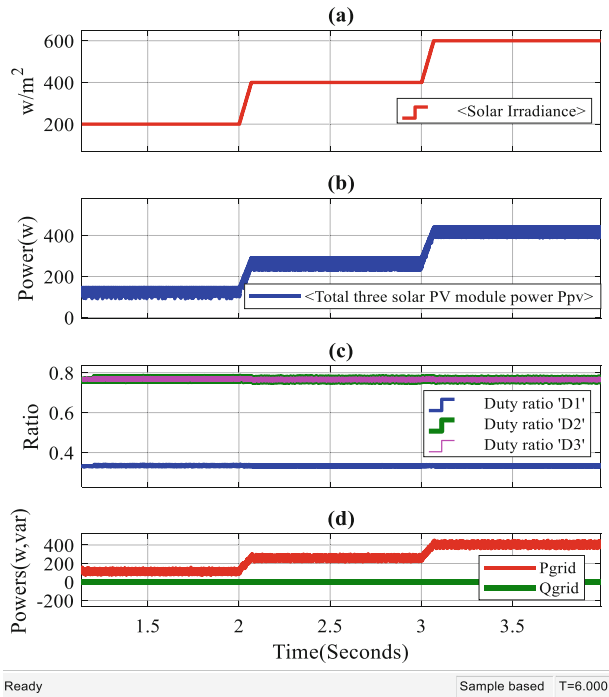


Fig. 6. (a) Solar Irradiance (b) Total power generated by three solar panels (c) Boost converter's Duty ratios (d) Active(P_{grid}) and reactive(Q_{grid}) power exporting to the grid

To export the power to the grid, the THD value of the current is necessary to maintain within IEEE standards. Figure 7(d) shows that at 200 w/m², 400 w/m², and 600 w/m² of

solar irradiance, the THD value of the current is 4.5%, 4%, and 3.5%, respectively. The asymmetrical inverter can export the 0.45 A of peak current at 200 w/m^2 irradiance, 1.7 A of peak current at 400 w/m^2 and 1.9 A of peak current at 600 w/m^2 to the grid shown in Fig. 7(c).

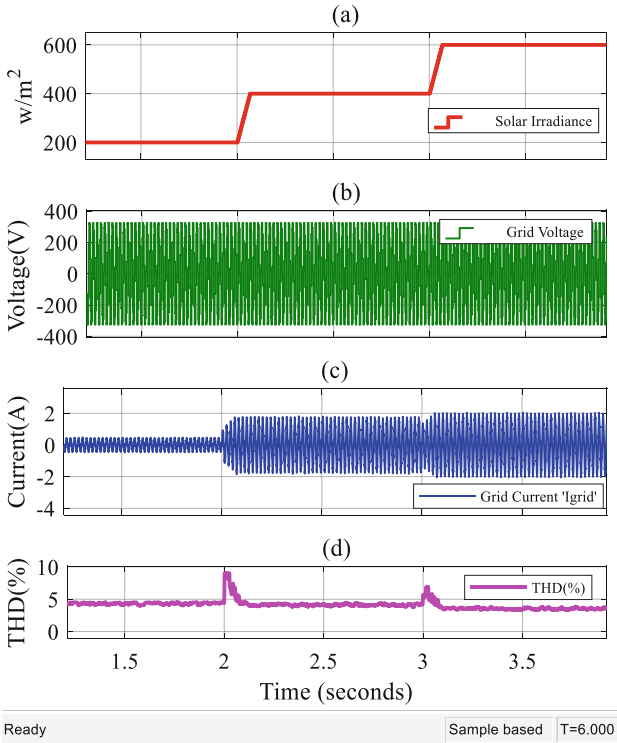


Fig. 7. (a) Solar Irradiance (b) grid voltage ' V_{grid} ' (c) grid current ' I_{grid} ' (d) grid current THD value in percentage

4.2 A Subsection Sample Proposed System Performance when Solar Irradiance Increases from 1000 W/m^2 to 600 W/m^2

The solar power output decreased from 720 W to 580 W at $t = 2$ s as the solar irradiance decreased from 1000 w/m^2 to 800 w/m^2 . The asymmetrical inverter can export 720 W at 1000 w/m^2 of radiation and 580 W at 800 w/m^2 to the grid depicted in Fig. 8(d). At $t = 3$ s, solar power generation increased from 580 W to 441 W as solar irradiance decreased from 800 w/m^2 to 600 w/m^2 , and the inverter exported the same amount of power to the grid. It has been noted that the inverter can export power to the utility grid as the solar irradiance rises.

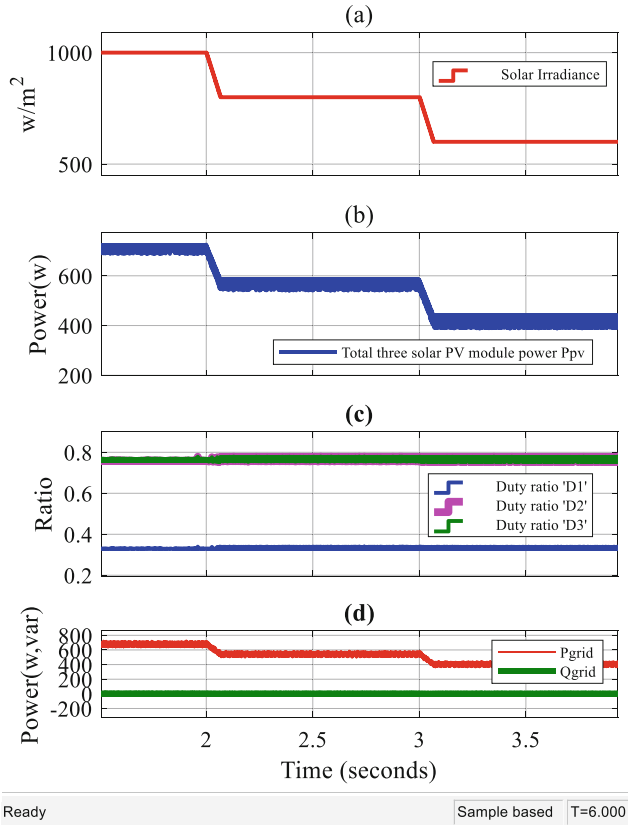


Fig. 8. (a) Solar Irradiance (b) Total power generated by three solar panels (c) Boost converter's Duty ratios (d) Active (P_{grid}) and reactive (Q_{grid}) power exporting to the grid.

To export the power to the grid, the THD value of the current is necessary to maintain within IEEE standards. The THD value of the current is 3%, 3.2%, and 3.5%, respectively, at 1000 w/m^2 , 800 w/m^2 , and 600 w/m^2 of solar irradiance, as shown in Fig. 9(d). The grid in Fig. 9(c) can receive peak currents of 2.75 A at 1000 w/m^2 irradiance, 2.35 A at 600 w/m^2 , and 1.9 A at 600 w/m^2 from the asymmetrical inverter.

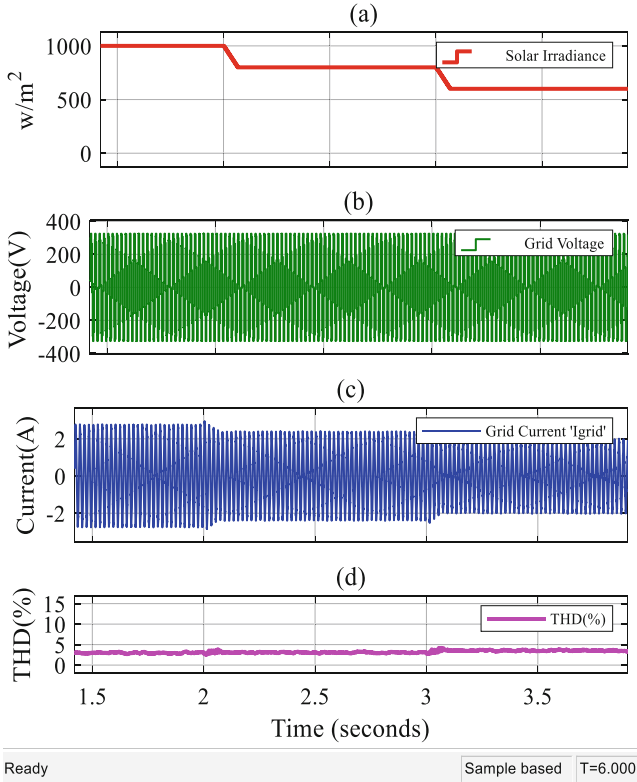


Fig. 9. (a) Solar Irradiance (b) grid voltage ' V_{grid} ' (c) grid current ' I_{grid} ' (d) grid current THD value in percentage

5 Conclusion

This work proposed the implementation of a fifteen-level inverter for PV applications. Conventional boost converters generate the required DC voltages, which are fed to the inverter for an AC stepped output waveform. The boost converters are designed to maintain the required output DC voltages for the inverter to function properly. The proposed system was tested under various solar irradiance conditions, and under all of them, the inverter performed better and could export power to the utility grid. When the solar irradiance increased and decreased, the inverter performed better. The inverter produces higher output voltage levels with fewer circuit components and low THD. The proposed system can export power to the grid while meeting IEEE standards in all solar irradiance conditions.

References

1. Pareek, P., Maurya, N.K., Singh, L., Gupta, N., Reis, M.J.C.S.: Study of smart city compatible monolithic quantum well photodetector. In: Gupta, N., Pareek, P., Reis, M. (eds.) *Cognitive Computing and Cyber Physical Systems 2022*, LNCS, vol. 472, pp. 215–224. Springer, Cham (2022)
2. Siva, A., Rajendran, V.: A novel auxiliary unit based high gain DC-DC converter for solar PV system with MPPT control. *Int. J. Power Electron. Drive Syst. (IJPEDS)* **13**, 2386–2395 (2022)
3. Bouaouaou, H., Lalili, D., Boudjerda, N.: Model predictive control and ANN-based MPPT for a multi-level grid-connected photovoltaic inverter. *Electr. Eng.* **104**, 1229–1246 (2022)
4. Siva, A., Rajendran, V.: A Novel asymmetric multilevel inverter with reduced number of switches for grid-tied solar PV system. *Recent Adv. Electr. Electr. Eng.* **15**, 379–389 (2022)
5. Sathiyathan, M., Jaganathan, S. and Josephine, R.L.: Multi-input and multi-output bi-directional power converter for solar photovoltaic system. *Electr. Eng.* **103**, 3201–3216 (2021)
6. Marimuthu, M., Vijayalakshmi, S., Shenbaga, L.R.: A novel non-isolated single switch multilevel cascaded DC–DC boost converter for multilevel inverter application. *J. Electr. Eng. Technol.* **15**, 2157–2166 (2020)
7. Chappa, A., Gupta, S., Sahu, L.K., Gupta, K.K.: Resilient multilevel inverter topology with improved reliability. *IET Power Electron.* **13**, 3384–3395 (2020)
8. Hwang, J., Lim, S., Choi, M.: Reactive power control method for grid-tie inverters using current measurement of DG output. *J. Electr. Eng. Technol.* **14**, 603–612 (2019)
9. Zhao, L., Song, W. and Feng, J.: A compensation method of dead-time and forward voltage drop for inverter operating at low frequency. *J. Electr. Eng. Technol.* **14**, 781–794 (2019)
10. Liu, G., Caldognetto, T., Mattavelli, P.: Power-based droop control in DC microgrids enabling seamless disconnection from AC grids. In: *IEEE Second International Conference on DC microgrids (ICDCM)*. IEEE, pp. 523–528 (2017)
11. Sharma, S., and Deshpande, A.: Design and development of maximum power point tracking algorithm using field programmable gate array. In: *2017 2nd IEEE International Conference on Recent Trends in Electronics, Information & Communication Technology (RTEICT)*, pp. 1560–1563 (2017)
12. Mantilla, M., Quinones, G., Castellanos, C., Petit, J., Ordonez, G.: Analysis of maximum power point tracking algorithms in DC–DC boost converters for grid-tied photovoltaic systems. In: *Annual Conference of the IEEE Industrial Electronics Society*, pp. 1971–1976 (2014)